JOURNAL OF MATERIALS SCIENCE 26 (1991) 2076 - 2080

Phase equilibria in ternary RE–Si–N systems (RE=Sc, Ce, Ho)

F. WEITZER, J. C. SCHUSTER
Institut für physikalische Chemie, Univis'tät Wien, Währingerstrasse 42, A-1090 Wien, Austria

J. BAUER, B. JOUNEL
Institute de Métallurgie, INSA Rennes, 20 Avenue Buttes de Coësmes, F-35043 Rennes, France

Phase equilibria in the ternary systems Sc–Si–N, Ce–Si–N and Ho–Si–N at 1000 °C and the binary boundary system Ho–Si are investigated. No new binary or ternary phases are found. In all three systems the respective rare-earth mononitride dominates the ternary phase fields and, with the exception of $HoSi_2$ in the Ho–Si–N system, coexists with all binary silicides. Thus Si_3N_4 is decomposed in contact with either scandium, cerium or holmium with the formation of ScN + $ScSi_{2-x}$, CeN + $CeSi_2$ and HoN + $HoSi_{2-x}$, respectively.

1. Introduction

Besides the existence of the two ternary phases $LaSi_3N_5$ [1, 2] and $Sm_3Si_6N_{11}$ [3] no data exist in the literature on ternary rare-earth metal–silicon–nitrogen systems. However, the binary systems RE–Si are established sufficiently to distinguish three groups of systems, each characterized by the occurrence and crystal structures of the intermediate phases (Fig. 1, Table I). Thus within a series of investigations of metal–silicon–nitrogen systems [4–7], one rare-earth metal of each group is chosen and the phase equilibria of the corresponding ternary systems are investigated as representative for the respective group: Ce–Si–N for group I (La, Ce, Pr and Nd); Ho–Si–N for group II (Sm, Gd, Tb, Dy, Ho, Er and Y); Sc–Si–N for group III (Tm, Yb, Lu and Sc).

2. Experimental procedure

Binary and ternary alloys were prepared from powders using Si (powder, purity 99.9%, Alpha Division, Ventron Corp., USA), Sc (pieces, purity 99.99%, Rare-Earth Products Ltd, UK), Ce (ingot, purity 99.9%, Rare-Earth Products Ltd,), Ho (powder, purity 99.9%, Alpha Division) and Si_3N_4 powder (mixture of α-Si_3N_4 and β-Si_3N_4, Si content 53%, Alpha Division). Appropriate mixtures of rare-earth metal and silicon were cold compacted and arc melted to prepare master alloys which were powdered (in the case of Ce alloys under a controlled atmosphere) and mixed with Si_3N_4 powder. Compacts of these mixtures were wrapped in Mo foil, sealed in evacuated quartz tubes and sintered at 1000 °C up to 1000 h. These alloys were water quenched and examined by X-ray diffraction (Cu$K\alpha_1$ radiation) using Guinier–Huber as well as 116 mm radius Debye–Scherrer cameras.

3. Results and discussion

3.1. Scandium–silicon–nitrogen system

The three binary intermediate phases $ScSi_{2-x}$ [8] (or Sc_3Si_5), ScSi [9] and Sc_5Si_3 [10] are corroborated to exist at 1000 °C. The crystal structures and lattice parameters found are in excellent agreement with the values reported. However, the phase $ScSi_{2-x}$ is not observed after prolonged annealing at 800 °C. At this temperature ScSi coexists with Si, at variance with the proposed phase diagram [11].

No ternary phase is found in the Sc–Si–N system. At 1000 °C, Si_3N_4 reacts with up to 45 at % Sc to form $ScSi_{2-x}$ and ScN (Table II), the only intermediate phase reported for the binary system Sc–N [12]. ScN coexists furthermore with ScSi and Sc_5Si_3 (Fig. 1). Owing to the decomposition of $ScSi_{2-x}$ at temper-

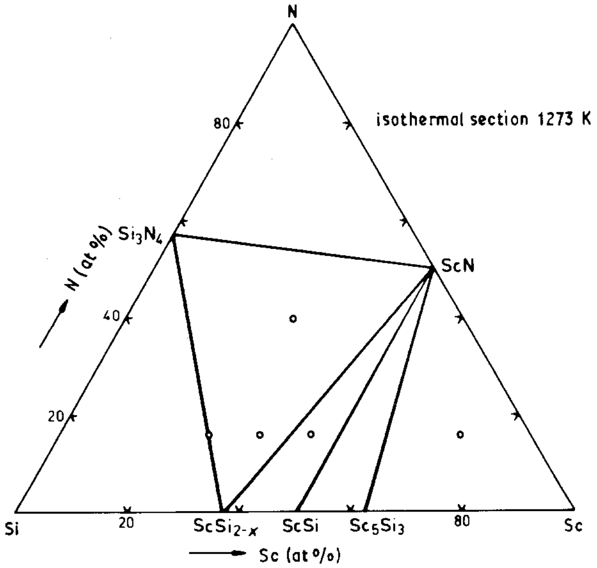

Figure 1 Isothermal section of the Sc–Si–N system at 1000 °C.

0022-2461/91 $03.00 + .12

TABLE I Classification of the binary systems RE–Si according to occurrence and crystal structure of the intermediate phases (the systems Eu–Si and Pm–Si are not included, because the data available are not sufficient for classification)

Group	Element	$RESi_2$		$RESi_{2-x}$ (RE_5Si_3)	RESi		RE_5Si_4	RE_5Si_3
I	La	$GdSi_2$-type	$ThSi_2$-type		FeB-type		Zr_5Si_4-type	Cr_5B_3-type
	Ce							
	Pr							
	Nd							
II	Sm			defect-AlB_2-type			Sm_5Ge_4-type	Mn_5Si_3-type
	Gd							
	Tb					CrB-type		
	Dy							
	Ho							
	Er							
	Y							
III	Tm							
	Yb							
	Lu							
	Sc							

TABLE II Solid state reaction products observed in the system Sc–Si–N upon annealing at 1000 °C for 170 h (in evacuated quartz tubes)

Si_3N_4 + 30 at % Sc	⟶	Si_3N_4 + ScN	(water quenched)
	⟶	Si_3N_4 + ScN + Si	(slow cooling)
Si_3N_4 + 72 at % Sc	⟶	Sc_5Si_3 + ScN	
$Sc_{0.375}$ $Si_{0.625}$ + Si_3N_4 (16 at % N)	⟶	$ScSi_{2-x}$ + Si_3N_4	(water quenched)
	⟶	ScN + ScSi + Si	(slow cooling)
$Sc_{0.50}$ $Si_{0.50}$ + Si_3N_4 (16 at % N)	⟶	$ScSi_{2-x}$ + Si_3N_4 + ScN	(quenched)
	⟶	ScN + ScSi + Si	(slow cooling)
$Sc_{0.675}$ $Si_{0.325}$ + Si_3N_4 (16 at % N)	⟶	ScSi + ScN	(+ unreacted Si_3N_4)

atures below 1000 °C > T > 800 °C, additional phases are repeatedly observed in air-quenched specimens, which indicates that ScN dominates completely the phase equilibria below 1000 °C > T > 800 °C, e.g. at 800 °C (Fig. 2).

3.2. Cerium–silicon–nitrogen system

The binary phase diagram Ce–Si, originally due to Benesovsky *et al.* [13], and updated by Gschneidner and Verkade [14], was reassessed by Munitz *et al.* [15]. The six intermediate phases reported to exist at 1000 °C are corroborated in the present investigation: $CeSi_2$ ($I4_1amd$, $ThSi_2$-type, $a = 0.4189$ nm, $c = 1.3892$ nm); $CeSi_{2-x}$ (Imma, $GdSi_2$-type, $a = 0.4195$ nm, $b = 0.4123$ nm, $c = 1.3905$ nm); CeSi (Pnma, FeB-type, $a = 0.8302$ nm, $b = 0.3965$ nm, $c = 0.5967$ nm); Ce_5Si_4 ($P4_12_12$ or $P4_32_12$, Zr_5Si_4-type, $a = 0.7949$ nm, $c = 1.5069$ nm); Ce_3Si_2 (P4/mbm, U_3Si_2-type, $a = 0.7800$ nm, $c = 0.4365$ nm) and Ce_5Si_3 (I4/mcm, Cr_5B_3-type, $a = 0.7896$ nm, $c = 1.3722$ nm).

No ternary phase is observed at 1000 °C in the Ce–Si–N system in the absence of external nitrogen pressure (Table III). Si_3N_4 reacts with up to 40 at % Ce to form $CeSi_2$ and CeN the only binary cerium nitride [16]. CeN coexists with all six binary cerium silicides (Fig. 3). The lattice parameters of the binary phases do not change upon equilibration with the respective third component indicating negligible solubility for it.

3.3. Holmium–silicon–nitrogen system

Because no proposal exists for the constitution of the binary boundary system holmium–silicon, a tentative phase diagram is compiled (Fig. 4) from X-ray (Table

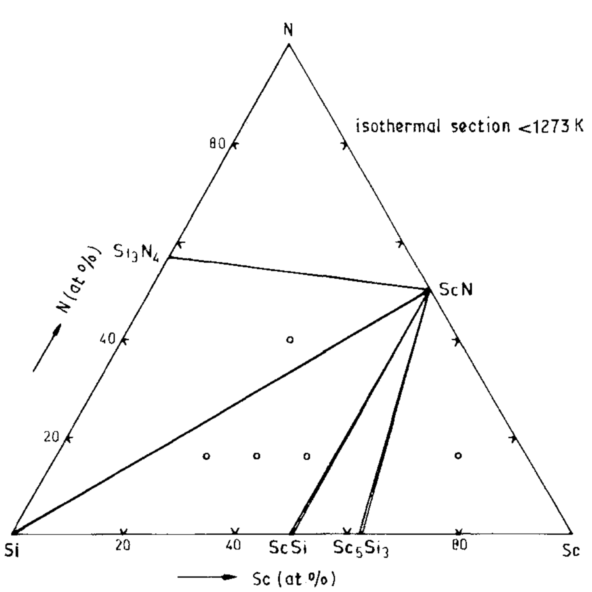

Figure 2 Isothermal section of the Sc–Si–N system at 800 °C.

TABLE III Solid state reaction products observed in the system Ce–Si–N upon annealing at 1000 °C for 240 h (in evacuated quartz tubes)

Si_3N_4 + 25 at % Ce	$\longrightarrow$	$CeN + CeSi_2 + Si_3N_4$	
Si_3N_4 + 52 at % Ce	$\longrightarrow$	$CeN + Ce_5Si_4$	
$Ce_{0.825}Si_{0.175} + Si_3N_4$ (16 at % N)	$\longrightarrow$	$CeN + Ce_5Si_3 + Ce$	
$Ce_{0.60}Si_{0.40} + Si_3N_4$ (8 at % N)	$\longrightarrow$	$CeN + Ce_5Si_4 + CeSi$	
$Ce_{0.60}Si_{0.40} + Si_3N_4$ (20 at % N)	$\longrightarrow$	$CeN + CeSi_2 + CeSi_{2-x} + Si_3N_4$	(no equilibrium)
$Ce_{0.50}Si_{0.50} + Si_3N_4$ (11 at % N)	$\longrightarrow$	$CeN + CeSi_{2-x}$	
$Ce_{0.50}Si_{0.50} + Si_3N_4$ (20 at % N)	$\longrightarrow$	$CeN + CeSi_2 + CeSi_{2-x} + Si_3N_4$	(no equilibrium)
$Ce_{0.33}Si_{0.67} + Si_3N_4$ (20 at % N)	$\longrightarrow$	$Si_3N_4 + CeSi_2$	

TABLE IV Results of X-ray analysis of binary Ho–Si alloys

Ho (at %)	As-cast	Annealed 1600 °C, 5 h	Annealed 1000 °C, 660 h
15	$Si + HoSi_2$		
20	$Si + HoSi_2$		
25	$Si + HoSi_2$		$Si + HoSi_2$
33	$HoSi_2 + HoSi_{2-x}$		$HoSi_2 + HoSi_{2-x}$
35	$HoSi_2 + HoSi_{2-x}$		$HoSi_2 + HoSi_{2-x}$
37.5	$HoSi_{2-x}$		$HoSi_{2-x}$
39	$HoSi_{2-x}$ + HoSi (FeB)		
43		$HoSi_{2-x}$ + HoSi (FeB)	$HoSi_{2-x}$ + HoSi (FeB)
47.5	$HoSi_{2-x}$ + HoSi (FeB) + HoSi (CrB)		
50	$HoSi_{2-x}$ + HoSi (FeB) + HoSi (CrB)	HoSi (FeB)	HoSi (FeB) + HoSi (CrB)
52	HoSi (FeB) + HoSi (CrB)		
55	HoSi (CrB) + Ho_5Si_4 + trace Ho_5Si_3	HoSi (CrB) + Ho_5Si_4 + trace Ho_5Si_3	
57.5	HoSi (CrB) + Ho_5Si_4 + Ho_5Si_3		HoSi (CrB) + Ho_5Si_3
58	$Ho_5Si_4 + Ho_5Si_3$		
62.5	trace $Ho_5Si_4 + Ho_5Si_3$	Ho_5Si_3	
70	$Ho_5Si_3 + Ho$		
80	$Ho_5Si_3 + Ho$		
90	$Ho_5Si_3 + Ho$		

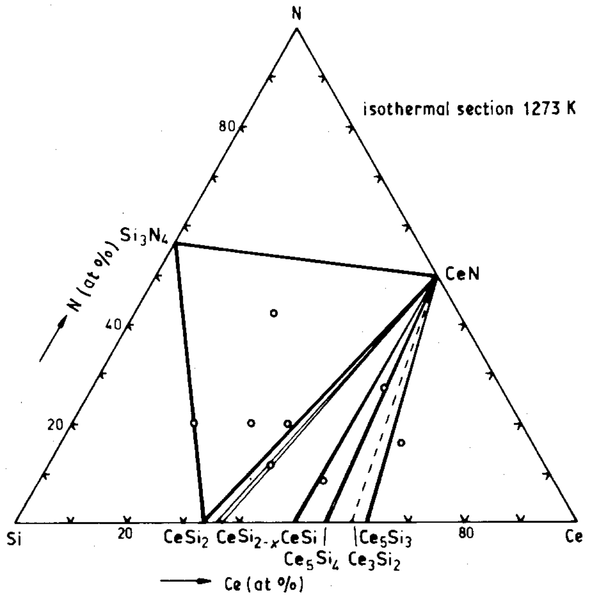

Figure 3 Isothermal section of the Ce–Si–N system at 1000 °C.

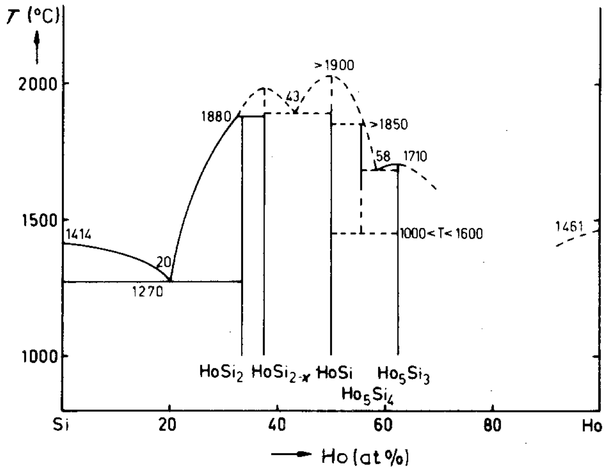

Figure 4 Tentative phase diagram of the binary Ho–Si system.

IV), metallographic and melting point data. All six intermediate phases reported in the literature are corroborated with respect to crystal structures and lattice parameters (Table V). The eutectic reaction, $Si + HoSi_2 \rightleftharpoons$ liquid, occurs near 20 at % Ho at 1270 °C. This value is only in fair agreement with the value of 1185 °C and 27 at % Ho given by Losovskii and Koleznichenko [23]. $HoSi_2$ melts incongruently around 1880 °C. $HoSi_{2-x}$ and HoSi both melt congruently at $T > 1990$ °C. The eutectic, $HoSi_{2-x} + HoSi \rightleftharpoons$ liquid, occurs near 43 at % Ho. The FeB-type structure modification of HoSi was found in HoSi containing alloys consisting of less than 50 at % Ho; the CrB-type modification dominates Ho-rich HoSi alloys (Table IV). Thus a composition-dependent phase transition is more likely than a temperature-dependent transformation h-HoSi → r-HoSi. The phase Ho_5Si_4 is assumed to melt incongruently at $T > 1850$ °C and is found to decompose below $1600\,°C > T > 1000\,°C$ into HoSi (CrB-type) and

TABLE V Structural data of the intermediate phases in the system Ho–Si

Ho (at %)	Phase	Lattice parameters (nm)				Reference
		a	b			
33	$HoSi_2$ (Imma, $GdSi_2$-type)	0.402 8(1)	0.391 2(1)	1.328 7(5)	(coex. with Si)	Present work
		0.401 0(7)	0.391 2(6)	1.325 5(17)	(coex. with $HoSi_{2-x}$)	Present work
		0.403	0.392	1.329		[17]
		0.403	0.397	1.331		[17]
		0.399	0.394	1.330		[20]
> 33	$HoSi_{2-x}$ (P6/mmm, AlB_2-type)	0.381 48(6)		0.410 73(5)	(coex. with $HoSi_2$)	Present work
		0.380 42(6)		0.410 75(5)	(coex. with HoSi (FeB))	Present work
		0.381 6(3)		0.410 7(3)		[17]
50	HoSi (Pnma, FeB-type)	0.780 39(4)	0.379 95(4)	0.562 82(7)	(coex. with $HoSi_{2-x}$)	Present work
		0.780 9(4)	0.380 6(1)	0.563 7(2)	(coex. with HoSi (CrB))	Present work
		0.780 8	0.380 1	0.563 3		[17, 18]
		0.781	0.379	0.563		[17]
50	HoSi (Cmcm, CrB-type)	0.423 2(1)	1.043 2(3)	0.380 4(1)	(coex. with HoSi (FeB))	Present work
		0.422 9(1)	1.045 0(1)	0.380 8(2)	(coex. with Ho_5Si_4)	Present work
		0.422 8	1.042 9	0.380 1		[17, 18]
55	Ho_5Si_4 (Pnma, Sm_5Ge_4-type)	0.731 8(9)	1.444 2(15)	0.763 1(1)		Present work
		0.733 8(5)	1.444 9(5)	0.762 5(5)		[19]
62	Ho_5Si_3 ($P6_3$/mcm, Mn_5Si_3-type)	0.833 6(2)		0.623 8(5)	(coex. with HoSi (CrB))	Present work
63		0.835 6(1)		0.627 3(4)	(coex. with Ho)	Present work
		0.834		0.622		[17]
		0.834 1(3)		0.625 3		[21]
		0.830 3		0.622 4		[22]

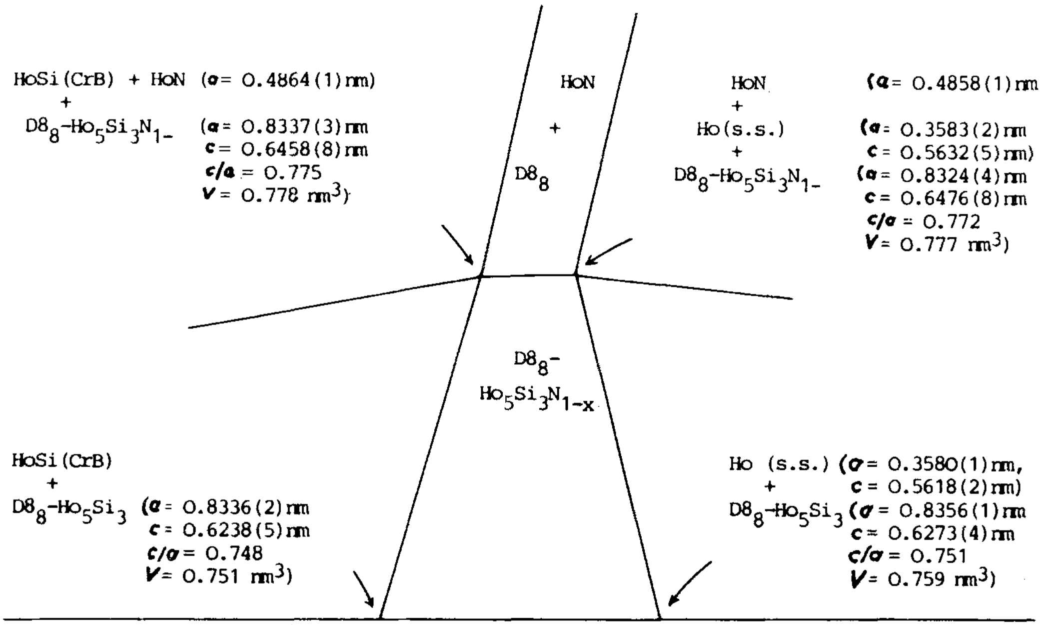

Figure 5 The phase field of the $D8_8$-phase $Ho_5Si_3N_{1-x}$ (schematic drawing).

Ho_5Si_3. The eutectic between Ho_5Si_4 and the congruent melting phase Ho_5Si_3 is near 58 at % Ho. The composition of the eutectic between Ho_5Si_3 and holmium could not be uniquely identified by the metallographic data of the present work.

No ternary phase is observed in the system Ho–Si–N at 1000 °C. Si_3N_4 reacts with up to 45 at % holmium to form $HoSi_{2-x}$ and HoN, the only holmium nitride existing in the binary Ho–N [24]. HoN coexists, in addition to $HoSi_{2-x}$, with HoSi and $Ho_5Si_3N_{1-x}$, which is formed by solid solution of nitrogen in binary Ho_5Si_3 as evinced by the increase of the lattice parameters (Fig. 5). HoSi in coexistence with $HoSi_{2-x}$ and HoN has FeB-type structure; HoSi coexisting with HoN and $Ho_5Si_3N_{1-x}$ crystallizes in the CrB-type structure. This supports the opinion, that the allotropy of HoSi is composition dependent. Lattice-parameter variations of Ho coexisting with $Ho_5Si_3N_{1-x}$ and HoN indicate a considerable solubility for nitrogen in holmium (Fig. 6).

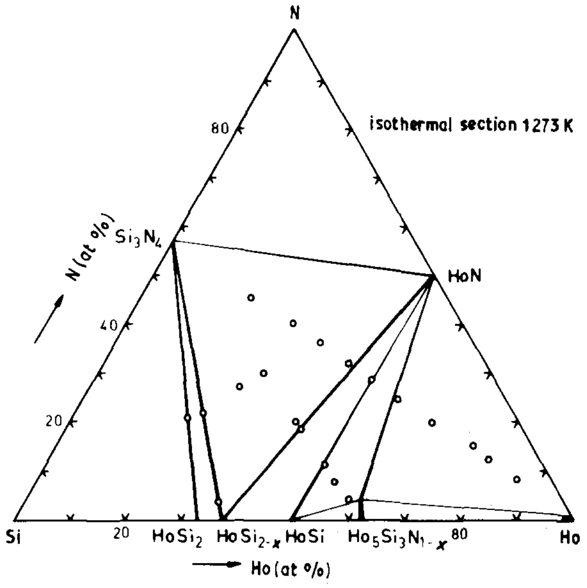

Figure 6 Isothermal section of the Ho–Si–N system at 1000 °C.

References

1. Z. INOUE, M. MITOMO and N. II, *J. Mater. Sci.* **15** (1980) 2915.
2. C. E. HOLCOMBE and L. KOVACH, *Ceram. Bull.* **60** (1981) 546.
3. J. GAUDÉ, J. LANG and D. LOUËR, *Rev. Chim. Miner.* **20** (1983) 523.
4. J. C. SCHUSTER, and H. NOWOTNY, Proceedings of the 11th International Plansee Seminar, Vol. 1, edited by H. Bildstein and H. M. Orlrer (Reutte, Austria, 1985) p. 899.
5. F. WEITZER and J. C. SCHUSTER, *J. Solid State Chem.* **70** (1987) 178.
6. F. WEITZER, P. ROGL and J. C. SCHUSTER, *Z. Metallkde* **79** (1988) 154.
7. J. C. SCHUSTER, *J. Mater. Sci.* **23** (1988) 2792.
8. O. SCHOB and E. PARTHÉ, *Monatsh. Chem.* **95** (1964) 1466.
9. *Idem., Acta Crystallogr.* **19** (1965) 214.
10. J. ARBUCKLE and E. PARTHÉ, *ibid.* **15** (1962) 1205.
11. A. B. GOKHALE and G. J. ABBASCHIAN, *Bull. Alloy Phase Diagr.* **7** (1986) 333.
12. R. P. ELLIOTT, "Constitution of Binary Alloys, 1st Supplement" (McGraw-Hill, New York, 1963).
13. F. BENESOVSKY, H. NOWOTNY, W. RIEGER and H. RAESSERTS, *Monatsh. Chem.* **97** (1966) 221.
14. K. A. GSCHNEIDNER and M. E. VERKADE, "Selected Cerium Phase Diagrams" (Rare Earth Information Center, Iowa State University, Ames, Iowa, 1974) Doc IS-RIC-7, p. 36 ff.
15. A. MUNITZ, A. B. GOKHALE and G. J. ABBASCHIAN, *Bull. Alloy Phase Diagr.* **10** (1989) 73.
16. G. F. KOBCHENKO and V. G. IVANTCHENKO, "Diagram. Sostoy. Metal. System" (Nauka, Moskow, 1971) p. 183; reproduced by W. G. MOFFATT in "The Handbook of Binary Phase Diagrams" (General Electric Comp., Schenectady, NY, 1976).
17. E. PARTHÉ, Colloqu. Int. CNRS No. 157, 1965 (CNRS, Paris, 1967) p. 195.
18. E. PARTHÉ, D. HOHNKE, W. JEITSCHKO and O. SCHOB, *Naturwiss.* **52** (1955) 155.
19. F. HOLTZBERG, R. J. GAMBINO and T. R. McGUIRE, *J. Phys. Chem. Solids* **28** (1967) 2283.
20. K. SEKIZAWA and K. YASUKCHI, *J. Phys. Soc. Jpn* **21** (1966) 274.
21. I. MAYER and I. FELNER, *J. Less-Common Metals* **29** (1972) 25.
22. D. I. TCHERNEV, K. S. S. L. NARASIMHAN and H. STEINFINK, *IEEE Trans Magn.* **5** (1969) 222.
23. V. N. LOZOVSKII and A. I. KOLESNICHENKO, *Izv. Akad. Nauk SSSR, Neorgan. Mater.* **17** (1981) 554.
24. G. BUSCH, P. JUNOD, O. VOGT and F. HULLIGER, *Phys. Lett.* **6** (1963) 79.

Received 27 October 1989
and accepted 24 April 1990